

ADAPTIVE ARRAY PROCESSING FOR WIDEBAND SONAR USING A CHIRP SOURCE

Qianjun Liu [†], Peter Ulriksen ^{††} and Geoffrey Shippey [†]

[†] Chalmers University of Technology, Dept. of Signals & Systems
GÖTEBORG, S412 96 SWEDEN.

^{††} Lund University of Technology, Dept. of Engineering Geology
LUND, S221 00 SWEDEN.

ABSTRACT

Adaptive array processing methods such as MUSIC, ESPRIT and WSF have played an important role in sonar and radar for target location and signal separation. However the emphasis has been on passive rather than active systems, and most algorithms are restricted to narrowband signals, and discrete targets. On the other hand interest in wideband chirp sonar is steadily increasing, with few natural point targets. The paper describes a methodology for bringing these fields together. After a wavefront alignment procedure based on quadrature match filtering, it is possible to derive a covariance matrix for each interesting angle of arrival with similar properties to the narrowband covariance matrix. Algorithms based on the eigenstructure of the covariance matrix can now be applied into wideband echoes with minimal modification. The paper presents results from simulation studies as well as field experimental data obtained across a 75m test site in Malmö Harbour.

1. INTRODUCTION

One advantage of wideband signals is well known: more acoustical energy can be projected into the water using a long pulse length without sacrificing range resolution. It was also found that wideband signals could be processed as simply as narrowband provided the spectrum of transmitted pulse is symmetric about the mid-frequency [1].

Sonar images can be generated by some form of time delay (e.g. phased array) beamsteering [2]. This conventional beamforming technique is inadequate for many purposes. Synthetic Aperture Sonar (SAS) [3, 4] is analogous to Synthetic Aperture Radar (SAR), which is now a routine method for obtaining high resolution radar imagery. However there is still a long way to go before SAS becomes routine. Positioning within a fraction of acoustical wavelength is difficult unless long acoustical wavelengths are used, which itself brings disadvantages for high resolution. Adaptive algorithms are an alternative way to improve angular resolution [5, 6, 7]. These include subspace methods, which decompose the received signal space into a source signal subspace and a noise subspace. By assuming the source signal subspace is orthogonal to the noise subspace, DOAs (directions of arrival) are determined at angles where the distance between a steering vector of that angle and noise subspace is a local minimum. These directions appear as local peaks in the spatial spectrum method. Unfortunately the DOA spectrum in subspace methods does not directly indicate signal strength. This is usually uninteresting for communication, but very important for sonar imaging. Hence some method of incorporating target strength estimation is needed to generate sonar images using subspace methods.

ADAPTIVE ARRAY PROCESSING FOR WIDEBAND SONAR

We propose here a new method for wideband active sonar array processing and imaging. This uses the MUSIC algorithm to estimate the DOA of reflectors and then converts the power of the echo from each reflector into the appropriate pixel intensity. Although MUSIC is the algorithm adopted in this paper, the methodology for extending array processing from narrowband to wideband should also be applicable to other adaptive array processing algorithms such as ML, ESPRIT and SWF.

2. THEORETICAL MODEL

In this section, the basic elements of wideband array processing and imaging are discussed. The relevant narrowband theory can be found in [5-8].

2.1 Signal model

Consider M incident signals $s_i(t)$ from different direction θ_i , $i = 1, 2, \dots, M$ are intercepted at time t by a uniform linear array (ULA) with L receiving elements. The received signal vector $\mathbf{x}(t)$ can be modelled as:

$$\mathbf{x}(t) = \mathbf{A}\mathbf{s}(t) + \mathbf{n}(t), \quad (1)$$

where $\mathbf{s}(t) = [s_1(t), s_2(t), \dots, s_M(t)]^T$, $\mathbf{x}(t) = [x_1(t), x_2(t), \dots, x_L(t)]^T$ and $\mathbf{n}(t) = [n_1(t), n_2(t), \dots, n_L(t)]^T$, with $x_l(t)$ and $n_l(t)$, $l = 1, 2, \dots, L$ denoting received signal and additive noise at channel l , respectively. $\mathbf{A} = [\mathbf{a}(\theta_1), \mathbf{a}(\theta_2), \dots, \mathbf{a}(\theta_M)]$, with $\mathbf{a}(\theta_i) = [1, e^{-j2\pi d \sin \theta_i}, \dots, e^{-j2\pi d(L-1) \sin \theta_i}]^T$ is the steering vector corresponding to θ_i , and d is the element separation in wavelengths. The following assumptions are used throughout this paper:

- 1) $M < N$,
- 2) $s_i(t)$ are zero mean and uncorrelated,
- 3) $n_l(t)$ are spatially white, and uncorrelated with $s_i(t)$. They are independent, identically distributed (IID) with zero means and variances σ^2 .

In a wideband active system, only the output of quadrature match filtering $\mathbf{x}(t)$ with the transmitted pulse is used for processing. After match filtering, (1) becomes

$$\mathbf{x}_f(t) = \mathbf{A} \mathbf{s}_f(t) + \mathbf{n}_f(t), \quad (2)$$

where $\mathbf{x}_f(t)$, $\mathbf{s}_f(t)$ and $\mathbf{n}_f(t)$ are the match filtered outputs of $\mathbf{x}(t)$, $\mathbf{s}(t)$ and $\mathbf{n}(t)$, respectively. Choosing a linear swept frequency chirp as source pulse, the linear relationship between phase and time shift for $\mathbf{x}_f(t)$ is the same as for a narrowband signal at the mid-frequency [1]. $\mathbf{x}_f(t)$ can then be processed using standard narrowband methods. While $\mathbf{n}_f(t)$ is no longer white in the frequency domain, having the same bandwidth as the chirp source, it is still spatially white, and Assumption 3 is satisfied. The notation f for match filtering, and the time parameter t , will be omitted in the following discussion unless the reader could be confused.

The first assumption means that only the M strongest signals will be selected. The second one is reasonable for distributed targets in the active sonar scenario. Although

ADAPTIVE ARRAY PROCESSING FOR WIDEBAND SONAR

all reflected echoes originate from a common source, echoes from distributed targets are uncorrelated under the following conditions:

- 1) distribution and reflectivity of reflectors forming the targets are uncorrelated,
- 2) the data set chosen from $\mathbf{x}(t)$ is much longer than the compressed pulse.

2.2 Covariance estimation

Let $\mathbf{R}_{xx} = E\{\mathbf{x}\mathbf{x}^H\}$ be the covariance matrix of the array output signal, where H (Hermitian) denotes conjugate transpose. Then in discrete form an estimate of \mathbf{R}_{xx} is

$$\hat{\mathbf{R}}_{xx} = \frac{1}{K} \sum_{k=0}^{K-1} \mathbf{x}(k)\mathbf{x}(k)^H, \quad (3)$$

where $\mathbf{x}(k)$, $k = 0, 1, \dots, K-1$ is the sampled form of $\mathbf{x}(t)$. For a ULA it is clear that \mathbf{R}_{xx} should have Töplitz structure. As suggested in [7, p. 57], setting the value of diagonal elements to their averaged value is a method of imposing a Töplitz structure on $\hat{\mathbf{R}}_{xx}$ and improving the covariance estimate. This in turn should improve DOA estimation.

2.3 DOA estimation

From the assumptions in 2.1 and eq. (2) the covariance matrix of \mathbf{x} becomes

$$\mathbf{R}_{xx} = \mathbf{A}\mathbf{R}_{ss}\mathbf{A}^H + \mathbf{R}_{nn}, \quad (4)$$

where $\mathbf{R}_{ss} = E\{ss^H\}$ is the covariance matrix of s , and $\mathbf{R}_{nn} = E\{nn^H\} = \sigma^2\mathbf{I}$ is the covariance matrix of n . Eigendecomposition of \mathbf{R}_{xx} gives

$$\begin{aligned} \mathbf{R}_{xx} &= \mathbf{U}_{xx}\mathbf{\Lambda}_{xx}\mathbf{U}_{xx}^H \\ &= \mathbf{U}_{ss}\mathbf{\Lambda}_{ss}\mathbf{U}_{ss}^H + \mathbf{U}_{nn}\mathbf{\Lambda}_{nn}\mathbf{U}_{nn}^H \\ &= \mathbf{U}_{ss}\mathbf{\Lambda}_{ss}\mathbf{U}_{ss}^H + \sigma^2\mathbf{U}_{nn}\mathbf{U}_{nn}^H, \end{aligned} \quad (5)$$

where \mathbf{U}_{xx} , \mathbf{U}_{ss} and \mathbf{U}_{nn} are the respective eigenmatrices of \mathbf{R}_{xx} , \mathbf{R}_{ss} and \mathbf{R}_{nn} . $\mathbf{\Lambda}_{xx}$, $\mathbf{\Lambda}_{ss}$ and $\mathbf{\Lambda}_{nn}$ are diagonal matrices whose components are the eigenvalues corresponding to their respective eigenmatrix. Since the eigenvalues in $\mathbf{\Lambda}_{ss}$ are all larger than σ^2 , the estimated noise subspace $\hat{\Pi}_{nn}$ is then the space spanned by the eigenvectors in \mathbf{U}_{xx} corresponding to the $L-M$ smallest eigenvalues. The θ_i are found from the local maxima of the MUSIC pseudo-spectrum:

$$P(\theta) = \frac{\mathbf{a}^H(\theta)\mathbf{a}(\theta)}{\mathbf{a}^H(\theta)\hat{\Pi}_{nn}\mathbf{a}(\theta)}. \quad (6)$$

For distributed targets with small angle spread, there are usually two principal eigenvalues corresponding to each target direction [9][10]. To form the noise space for distributed targets, it is reasonable to select the number of noise eigenvectors according to this criteria.

ADAPTIVE ARRAY PROCESSING FOR WIDEBAND SONAR

2.4 Target strength estimation [8]

Although θ_i can be estimated more accurately by subspace based methods like MUSIC than by conventional beamforming, these methods cannot be applied immediately to sonar imaging. The MUSIC spectrum merely indicates the distance between the noise subspace and steering vector for the true DOA, whereas pixel brightness in a sonar image should represent the strength of the reflector (or reflectors) at the location corresponding to that pixel. From (4), we have

$$\mathbf{A}^H \mathbf{R}_{xx} \mathbf{A} = \mathbf{A}^H \mathbf{A} \mathbf{R}_{ss} \mathbf{A}^H \mathbf{A} + \sigma^2 \mathbf{A}^H \mathbf{A}, \quad (7)$$

and
$$\mathbf{R}_{ss} = (\mathbf{A}^H \mathbf{A})^{-1} \mathbf{A}^H \mathbf{R}_{xx} \mathbf{A} (\mathbf{A}^H \mathbf{A})^{-1} - \sigma^2 (\mathbf{A}^H \mathbf{A})^{-1}, \quad (8)$$

where
$$\mathbf{R}_{ss} = \begin{bmatrix} r_{s_1 s_1} & r_{s_1 s_2} & \dots & r_{s_1 s_M} \\ r_{s_2 s_1} & r_{s_2 s_2} & \dots & r_{s_2 s_M} \\ \vdots & \vdots & \ddots & \vdots \\ r_{s_M s_1} & r_{s_M s_2} & \dots & r_{s_M s_M} \end{bmatrix}, \text{ and } r_{s_i s_j} = E\{s_i s_j^*\} \quad i, j = 1, 2, \dots, M.$$

Taking the estimated DOA from (6) as the true DOA in (8), signal powers can then be estimated from the main diagonal of \mathbf{R}_{ss} . Eq (8) is also the Maximum Likelihood estimation of \mathbf{R}_{ss} if \mathbf{s} is a Gaussian signal vector. Expanding this equation shows that the i th element in the main diagonal of $\mathbf{A}^H \mathbf{R}_{xx} \mathbf{A}$ can be written:

$$\mathbf{a}(\theta_i)^H \mathbf{R}_{xx} \mathbf{a}(\theta_i) = \sum_{j=1}^M r_{s_j s_j} d_{ij} + \sigma^2 M^2, \quad i = 1, 2, \dots, M, \quad (9)$$

where $d_{ij} = \mathbf{a}^H(\theta_i) (\mathbf{a}(\theta_j) \mathbf{a}^H(\theta_j)) \mathbf{a}(\theta_i)$, $j = 1, 2, \dots, M$, and $d_{ii} = M^2$.

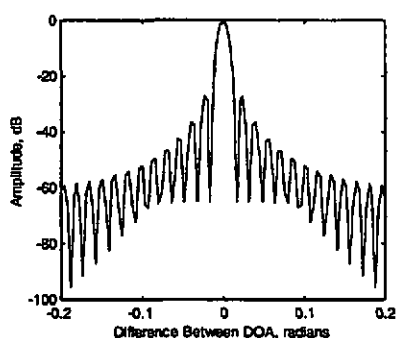


Fig. 1 d_{ij}/M^2 changes according to $\Delta\theta$, vertical axis: d_{ij}/M^2 , horizontal axis: $\Delta\theta$.
conventional beamformer. Otherwise they must be estimated from (8).

The left side of (9) is exactly the spectrum of a conventional beamformer. This equation shows that the conventional beamformer output is a weighted combination of noise power and signal powers from every direction, with the power from direction θ_i as the principal component. d_{ij} is the inverse of the distance between $\mathbf{a}(\theta_i)$ and the space spanned by $\mathbf{a}(\theta_j)$. Fig. 1 shows the relationship between d_{ij}/M^2 and $\Delta\theta = \theta_i - \theta_j$. The greater the separation of θ_j from θ_i , the less $r_{s_j s_j}$ contributes to the conventional beamformer output at θ_i . Provided signals are well separated, the signal powers are given by the output of a

ADAPTIVE ARRAY PROCESSING FOR WIDEBAND SONAR

3. SYSTEM DESCRIPTION

3.1 DAIM

Digital Acoustic IMaging (DAIM) is a collaborative project between Chalmers University of Technology (CTH) and Lund University of Technology (LTH). The main contribution from CTH is signal processing, while LTH has carried out the field experiments [11]. The aim of the DAIM project is high-resolution underwater sonar imaging using wideband insonification. A powerful 32 channel data recording system was built for experimental work by SubVision AB under contract to LTH. Experiments have been conducted from the quayside in quiet harbour waters with specially constructed targets placed on the harbour floor.

3.2 Image generation

Processing begins by match filtering the received echoes with a kernel set derived from a careful calibration experiment. Apart from achieving the required linear relationship between phase and time shift, this operation also compensates for channel variation and system response. To generate the polar image, pixels must be assigned a value which indicates the location and strength of reflectors. For each pixel, the 2-way time delay from transmitter to reflector and back to the centre of the receiver array is calculated and a certain length of data about this time delay is selected from the whole data sequence. The angular location and strength of possible targets is then estimated based on this windowed data set.

In general the wavefront of compressed wideband signals coming from large angles will not cover the whole receiver aperture at any time. Wavefront alignment is then needed before estimating the covariance matrix from the data [1]. However look angles used in these experiments were small, and this step was omitted. The modified MUSIC procedure for active sonar imaging, here termed MODMUSIC, was then as follows:

- 1) match filter $\mathbf{x}(t)$ with the kernel set of the array to get $\mathbf{x}_f(t)$,
- 2) let $[R_{min}, R_{max}, R_r, \theta_{min}, \theta_{max}, R_\theta]$ define the polar frame of the image area, with R_{min}, R_{max}, R_r and $\theta_{min}, \theta_{max}, R_\theta$ denoting minimum, maximum and number of pixels in range and azimuth.
- 3) for given $r \in [R_{min}, R_{max}]$ do
 - a) for given $\theta \in [\theta_{min}, \theta_{max}]$, align the wavefront of $\mathbf{x}_f(t)$ by this angle θ , and select a data set $\mathbf{d}(r, W)$, corresponding to r with a window length of W , from aligned $\mathbf{x}_f(t)$,
 - b) form MUSIC pseudo spectrum within $[\theta_{min}, \theta_{max}]$ by (6) using $\mathbf{d}(r, W)$,
 - c) select M highest peaks in this spectrum,
 - d) estimate signal strength for each peak using (8),
 - e) generate a Gaussian "spectrum" for the neighbourhood of each peak with the appropriate peak signal strength and add. The sd of the Gaussians is determined by the normal azimuth resolution attempted.
- 4) end of the procedure.

ADAPTIVE ARRAY PROCESSING FOR WIDEBAND SONAR

There are many other ways of modifying the normal MUSIC spectrum to take account of signal strength, but the above method seemed to be the simplest.

4. SIMULATION AND EXPERIMENTAL RESULTS

Fig. 2 shows simulation results of applying MODMUSIC to a scenario with two uncorrelated targets. The power of target 1 is 0.61 times the power of target 2. True DOAs are (0.00, 0.04) in Fig. 2a, and (0.00, 0.01) in Fig. 2b. Fig. 2a shows that the target strengths estimated from eq (8) are almost the same as from a conventional beamformer. However the conventional beamformer fails to resolve the two targets in Fig. 2b, while MODMUSIC correctly indicates both target locations and strengths.

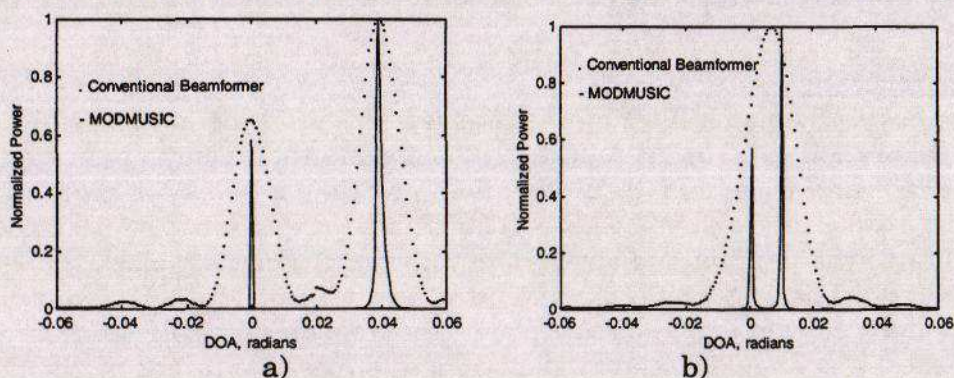


Fig. 2 Power spectrum of beamforming for targets, a) well separated, b) closely located.

Experimental data was obtained using a 32-channel receiver array with receiver elements spaced by 15mm. Images of three targets were generated by three different methods, viz. time delay beamforming, SAS with aperture length 4.3m, and MODMUSIC. To improve SNR and reduce randomness in targets reflectivity, images generated from 16 pings were averaged both in time delay beamforming and MODMUSIC. Fig. 3a shows the T-frame supporting styrofoam balls, 3-15cm in diameter, separated by 10-30cm. This was placed on the seabed at 17m range. Fig. 3b shows the step target of size 0.5m x 2.0m, placed at 21m range. Each face of the step target was coated with irregular plastic balls to achieve surface scattering. Fig. 3c shows the metal fence wall supporting the bank across the harbour, at a range of 75 meters.

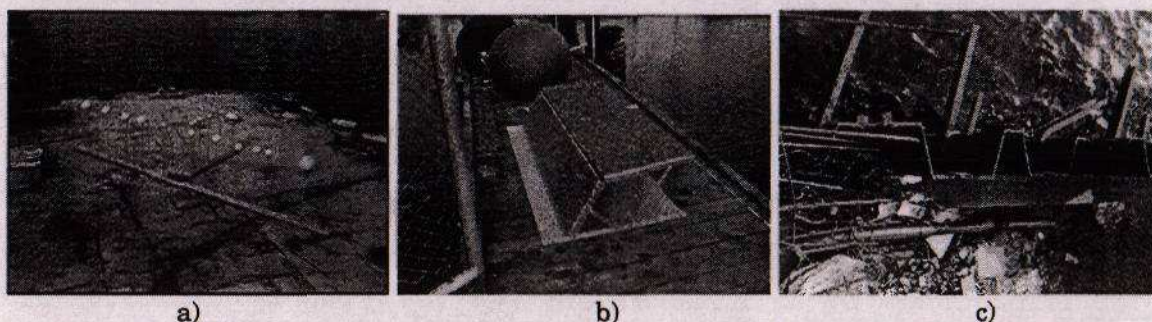


Fig. 3 Photographs of under water targets, a) T target, b) Step target, c) metal fence.

ADAPTIVE ARRAY PROCESSING FOR WIDEBAND SONAR

Fig. 4-6 are acoustic images of these targets. For the T-target the number of balls can be counted in the SAS image across the whole frame and in MODMUSIC on the left side of the image. The boundaries of the step target and metal fence are clear from both the MODMUSIC and SAS images. The resolution of both SAS and MODMUSIC images is much better than those of the time delay images. Slightly better resolution is achieved using SAS with an aperture 10 times longer than the MODMUSIC aperture.

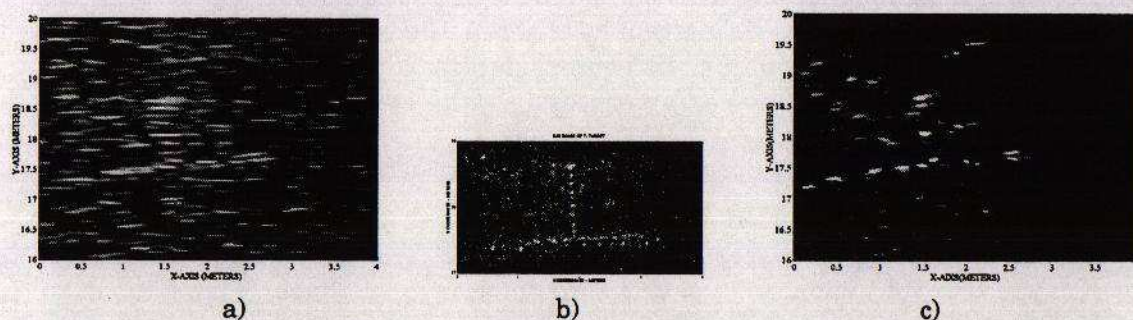


Fig. 4 T-target image with different methods, a) time delay, b) SAS, c) MODMUSIC.

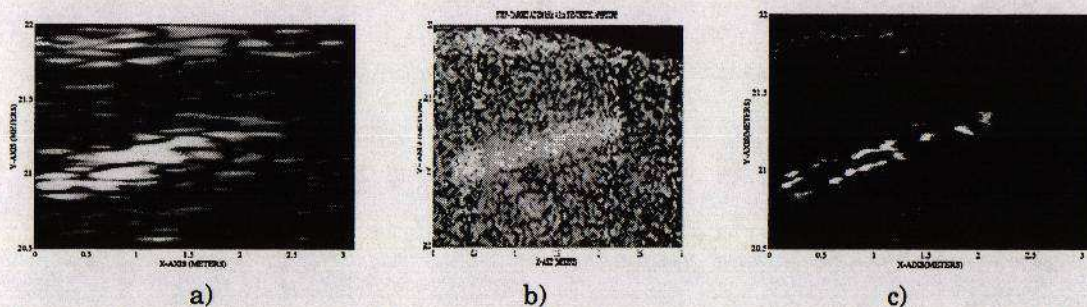


Fig. 5 Step-target image with different methods, a) time delay, b) SAS, c) MODMUSIC.

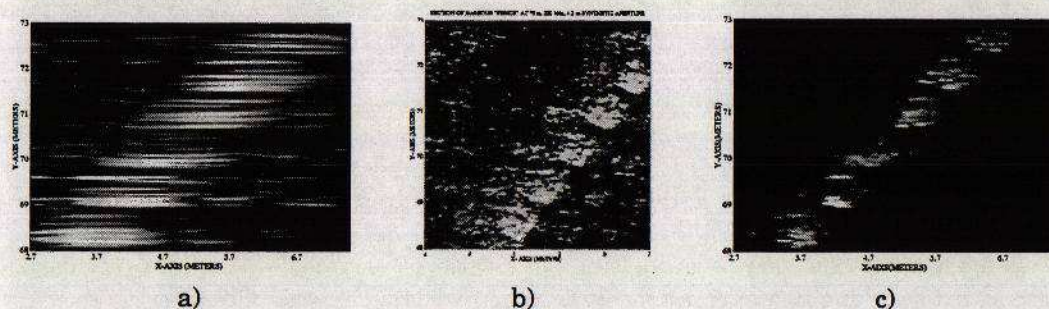


Fig. 6 Metal fence image with different methods, a) time delay, b) SAS, c) MODMUSIC.

ADAPTIVE ARRAY PROCESSING FOR WIDEBAND SONAR

5. CONCLUSIONS

We have presented an adaptive beamforming method for wideband active sonar imaging which improves angular resolution considerably. The method exploits the linear phase property of a match-filtered chirp echo, improved covariance matrix estimation, and MUSIC modified to indicate target strength. But this is still very basic. Improvements could be investigated at least in the following ways:

- 1) alternative models for distributed targets,
- 2) using image processing method to exploit target structure,
- 3) improved covariance estimation by other methods such as spatial smoothing,
- 4) improved DOA estimation with other adaptive algorithms,
- 5) combination of adaptive array processing with SAS.

6. ACKNOWLEDGMENTS

The DAIM project is supported by the Swedish State Board NUTEK. DYKMA AB provided valuable trials facilities in Malmö Harbour. The work of Per Gunnerson and Olle Kröling of SubVision AB, and Peter Jonsson and Claes Hovmalm of LTH in carrying out experiments is gratefully acknowledged.

7. REFERENCES

- [1] G. A. Shippey, P. Ulriksen and Q. Liu. Quasi-narrowband processing of wideband sonar echoes. In *Proc. 4th European Conference on Underwater Acoustics*, pages 63-68. Rome, Italy, September 1998.
- [2] R. O. Nielsen. *Sonar Signal Processing*. Artech House, 1991.
- [3] M. P. Hayes and P. T. Gough. Broad-band synthetic-aperture sonar. *IEEE J. Oceanic Eng.*, 17(1):80-94, 1992.
- [4] J. Chatillon, M. E. Bouthier and M.A. Zakharia. Synthetic aperture sonar for seabed imaging: relative merits of narrow-band and wide-band approaches. *IEEE J. Oceanic Eng.*, 17(1):95-105, 1992.
- [5] B. D. Van Veen and K. M. Buckley. Beamforming: A versatile approach to spatial filtering. *IEEE Signal Processing Magazine*, pages 4-24, April 1988.
- [6] H. Krim and M. Viberg. Two decades of array signal processing research: The parametric approach. *IEEE Signal Processing Magazine*, pages 67-94. July 1996.
- [7] S. Haykin, J. Litva, and T. J. Shepherd (eds.). *Radar Array Processing*. Springer Verlag, Berlin, 1993.
- [8] R. O. Schmidt. A signal subspace approach to multiple emitter location and spectral estimation. Ph.D. thesis, Stanford University, Stanford, CA, November 1981.
- [9] T. Trump and B. Ottersten. Estimation of nominal direction of arrival and angular spread using an array of sensors. *Signal Processing*, 50(1-2):57-69, April 1996.
- [10] M. Bengtsson. Sensor array processing for scattered sources. Licentiate Thesis, Dept. of Signals, Sensors, and Systems, KTH, Stockholm, Sweden, December 1997.
- [11] G. A. Shippey, P. Ulriksen and Q. Liu. Wideband swath bathymetry, SAS autofocus and underwater navigation fixes: three related problems in echo/image correlation. To appear in *Proc. Int. Conf. on Sonar Signal Processing*. Weymouth, UK, December 1998.